



Department of Electrical and Computer Engineering

North South University

Directed Research

**Segmentation of Blood Vessels, Optic Disc Localization, Exudate Detection for
Diabetic Retinopathy, and Glaucoma Diagnosis from Fundus Images**

Md. Marop Hossain

ID# 2013982042

Md. Zunayed Islam Pranto

ID# 1921609042

Faculty Advisor:

Dr. Mohammad Ashrafuzzaman Khan

Assistant Professor

ECE Department

Spring, 2024

APPROVAL

Md. Marop Hossain (ID # 2013982042), **Md. Zunayed Islam Pranto** (ID # 1921609042) from Electrical and Computer Engineering Department of North South University, have worked on the Directed Research Project titled “**Segmentation of Blood Vessels, Optic Disc Localization, Exudate Detection for Diabetic Retinopathy, and Glaucoma Diagnosis from Fundus Images**” under the supervision of **Dr. Mohammad Ashrafuzzaman Khan** partial fulfillment of the requirement for the degree of Bachelors of Science in Engineering and has been accepted as satisfactory.

Supervisor’s Signature

.....

Dr. Mohammad Ashrafuzzaman Khan

Assistant Professor

Department of Electrical and Computer Engineering

North South University

Dhaka, Bangladesh.

Chairman’s Signature

.....

Dr. Rajesh Palit

Professor

Department of Electrical and Computer Engineering

North South University

Dhaka, Bangladesh.

DECLARATION

This is to declare that this project/directed research is our original work. No part of this work has been submitted elsewhere partially or fully for the award of any other degree or diploma. All project related information will remain confidential and shall not be disclosed without the formal consent of the project supervisor. Relevant previous works presented in this report have been properly acknowledged and cited. The plagiarism policy, as stated by the supervisor, has been maintained.

Students' names & Signatures

1. Md. Marop Hossain

2. Md. Zunayed Islam Pranto

ACKNOWLEDGEMENTS

The authors would like to express their heartfelt gratitude towards their project and research supervisor, **Dr. Mohammad Ashrafuzzaman Khan**, Assistant Professor, Department of Electrical and Computer Engineering, North South University, Bangladesh, for his invaluable support, precise guidance and advice pertaining to the experiments, research and theoretical studies carried out during the course of the current project and also in the preparation of the current report.

Furthermore, the authors would like to thank the Department of Electrical and Computer Engineering, North South University, Bangladesh for facilitating the research. The authors would also like to thank their loved ones for their countless sacrifices and continual support.

ABSTRACT

Segmentation of Blood Vessels, Optic Disc Localization, Exudate Detection for Diabetic Retinopathy, and Glaucoma Diagnosis from Fundus Images

Diabetic Retinopathy is a complication of long-standing unchecked diabetes; untreated Diabetic Retinopathy causes harm to retinal blood vessels, resulting in visual deficiency. Glaucoma is a group of eye conditions. Untreated Glaucoma results in damaged optic nerve and even vision loss. This paper focuses on methods to extract some of the key features, such as blood vessels, optic disc, and exudates, that may help detection of both Diabetic Retinopathy and Glaucoma at an early stage. Vessel segmentation was performed with a less computational, unsupervised auto-mated technique performed on an openly accessible Structured Analysis of the Retina dataset containing 400 raw images and 44 cited images marked by experts. Detection is done through a morphological hessian approach and region-based Otsu thresholding. Further enhancement was done by performing the Histogram Equation, hessian matrix, and eigenvalues approach. Optic Disc and Exudates detection was performed on a publicly available Indian Diabetic Retinopathy Image Dataset. Optic Disc and Exudates segmentation was performed using k-means clustering and template matching. Both methods achieved high accuracy in performing the segmentation of blood vessels, optic disc localization, and detection of exudates. These results can be highly beneficial in detecting Diabetic Retinopathy and Glaucoma at an early stage.

TABLE OF CONTENTS

APPROVAL	i
DECLARATION	ii
ACKNOWLEDGEMENTS	iii
ABSTRACT.....	iv
TABLE OF CONTENTS.....	v
LIST OF FIGURES	vii
LIST OF TABLES	viii
Chapter 1 Introduction	1
1.1 Background and Motivation.....	1
1.2 Purpose and Goal of the Project.....	2
1.3 Organization of the Report.....	3
Chapter 2 Research Literature Review	4
2.1 Existing Research and Limitations	4
Chapter 3 Methodology	6
3.1 System Design	6
3.1.1 Optic Disc Localization System Diagram.....	6
3.1.2 Exudates Detection System Diagram.....	7
3.1.3 Blood Vessel Segmentation System Diagram	8
3.1.4 Data collection	9
3.2 Hardware and/or Software Components	9
3.3 Hardware and/or Software Implementation.....	11
3.3.1 Localization of Optic Disc	11
3.3.2 Detection of Exudates	12
3.3.3 Vessel Segmentation.....	14

Chapter 4 Investigation/Experiment, Result, Analysis, and Discussion.....	19
4.1 Investigation/Experiment.....	19
4.2 Result	19
4.2.1 Localization of Optic Disc	19
4.2.2 Detection of Exudates	19
4.2.3 Segmentation of blood vessels.....	20
4.3 Analysis.....	22
4.4 Discussion	23
Chapter 5 Conclusions	24
8.1 Summary	24
8.2 Limitations	24
8.3 Future Improvement.....	25
References	26

LIST OF FIGURES

Fig. 1: Different features in a typical DR, Glaucoma affected image.....	01
Fig. 2: Optic Disc Localization Flow Diagram.....	06
Fig. 3: Exudates Detection Flow Diagram.....	07
Fig. 4: Segmentation Diagram.....	08
Fig. 5: (a) Original image.....(g) Masking OD region.....	12
Fig. 6: (a) Original Image.....(e) Final segmentation result after OD masking.....	13
Fig. 7: DCNN architecture... ..	13
Fig. 8: RGB Channel Splitting.....	14
Fig. 9: Applying CLAHE and Morphological Filter.....	16
Fig. 10: Applying Hessian Matrix.....	16
Fig. 11: Image Fusioning.....	17
Fig. 12: Local Otsu thresholding.....	17
Fig. 13: Pixel area-based Thresholding.....	18
Fig. 14: Optic Disc masked image (left) with the original image (right).....	19
Fig. 15: (a), (b) Result of proposed exudate detection... ..	20
Fig. 16: Segmentation result for the best case (left) with ground truth (right).....	20

LIST OF TABLES

Table 1: Hardware/Software components.....	09
Table 2: List of Software, Libraries and other's Tools.....	10
Table 3: Results of the proposed vessel segmentation method on the STATE dataset.....	20

Chapter 1 Introduction

1.1 Background and Motivation

Diabetic Retinopathy (DR) and Glaucoma are two of the most common and serious eye conditions. Diabetic Retinopathy is a direct consequence of prolonged, unchecked diabetes and Glaucoma is a group of eye conditions that damage the optic nerve, often due to abnormally high intraocular pressure. If untreated at an earlier stage both lead to vision loss and blindness at an early age. Globally, 600 million people will have diabetes by 2040, with a third having DR [1]. The global prevalence of glaucoma for people aged 40–80 is 3.4%, and by the year 2040 it is projected there will be approximately 112 million affected individuals worldwide [2]. Diabetic Retinopathy is a complication of diabetes, if diabetic patients blood sugar levels mostly remain high, prolonged high blood sugar levels cause damage to the retinal blood vessels, leading to leakage, swelling. In severe cases some research found growth of abnormal blood vessels. In case of glaucoma damage typically occurs gradually, with peripheral vision being affected first, which makes early detection difficult.

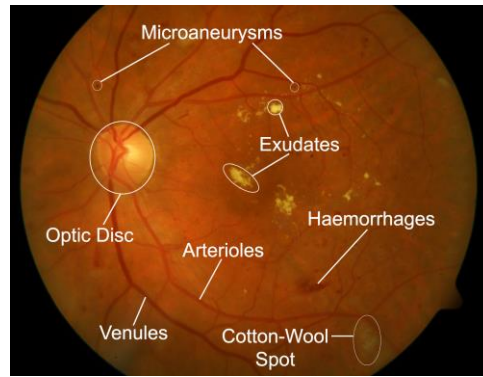


Fig. 1: *Different features in a typical DR, Glaucoma affected image*

Ophthalmologists identify Diabetic Retinopathy based on certain features viz. blood vessel area, soft and hard exudates, hemorrhages, cotton wool spots and microaneurysms as well as diagnose glaucoma by looking at specific indicators such as the cup-to-disc ratio, the thickness of the retinal nerve fiber layer, and changes in the optic disc's appearance. Automating the detection of these features from fundus images allows for quicker and earlier diagnosis of Diabetic Retinopathy and glaucoma.

1.2 Purpose and Goal of the Project

The project "Segmentation of Blood Vessels, Optic Disc Localization, Exudate Detection for Diabetic Retinopathy, and Glaucoma Diagnosis from Fundus Images" presents the development of an automated system for early detection and diagnosis of two of the most common yet potentially blinding eye conditions: Diabetic Retinopathy and Glaucoma. Glaucoma is a complex disease multiple factors are associated with glaucoma diagnosis. That is why traditional CNN models can not accurately direct Glaucoma. Accuracy is quite unreliable.

The primary objective is to utilize advanced image processing techniques and machine learning algorithms to accurately segment retinal blood vessels, localize the optic disc, and detect exudates from fundus images which gives an edge over traditional methods. Extracting multiple factors at a time assists medical professionals to diagnose Diabetic Retinopathy and Glaucoma far more accurately.

Contributions and Novelty

1. **Comprehensive Automated Diagnosis:** An automated way of segmentation of Blood Vessels from fundus images as well as Optic Disc Localization and Detection of Exudates gives ophthalmologists hint for potential protein leakage, thinning in blood vessel and abnormal Optic Disc related data to early diagnosis of Diabetic Retinopathy, and Glaucoma.
2. **Higher Precision and Early Detection:** Glaucoma is a complex disease multiple factors are associated with glaucoma diagnosis. Traditional CNN models can not accurately direct Glaucoma. This project performs multiple diagnostic tasks—such as blood vessel segmentation, optic disc localization, and exudate detection. This, therefore, is a one-stop system that can effectively diagnose Diabetic Retinopathy besides Glaucoma. Extracting multiple factors at a time assists medical professionals to diagnose Diabetic Retinopathy and Glaucoma far more accurately.
3. **Accessibility and Scalability:** The project has the potential to be implemented in a variety of healthcare centers, which includes remote or under-resourced areas, therefore extending the limits on the provision of crucial diagnosis services and screening programs.

4. **Novel Approach to Multi-Disease Detection:** This project aimed at addressing Diabetic Retinopathy and Glaucoma together under one diagnostic framework is unique in the field of ophthalmology; such a system could reduce the time and monetary expenses spent on multiple unilateral examinations.

Over all this project vision to offer third world countries like Bangladesh a cost-effective, very accurate, and hugely scalable automated tool for detecting Diabetic Retinopathy and Glaucoma furthering the cause of eradicating preventable blindness.

1.3 Organization of the Report

Chapter 2: Presents the literature reviews related to this project.

Chapter 3: Defines methodology of the project. Projects dataset, system designing, as well as the hardware and software components implementations.

Chapter 4: Presents the Investigation/Experiment, Result, Analysis and Discussion.

Chapter 5: Presents the defined conclusion of the project, limitations, and future possibilities.

Chapter 2 Research Literature Review

2.1 Existing Research and Limitations

The segmentation of retinal blood vessels, optic disc localization, exudate detection, diabetes retinopathy, and glaucoma diagnosis from Fundus pictures have all been actively explored in recent years, with major advances driven by deep learning and image processing technologies. Many strategies have been developed over the years to address this issue, each with its own set of benefits and drawbacks.

Segmenting blood vessels in retinal pictures is an important step in identifying many eye illnesses. However, problems such as changing vessel lengths, low contrast, and picture noise complicate this effort. A hierarchical strategy for segmenting retinal blood vessels, based on feature and ensemble learning, has been shown to improve accuracy and robustness in detecting vessels of various sizes [3]. This approach improves segmentation accuracy by combining a variety of factors such as intensity, edges, and texture, particularly in the refinement of vessel borders. Another technique uses multi-scale textons, which are microscopic texture patterns produced from key locations, to capture fine vessel details, particularly in low-contrast places [4]. This strategy surpasses traditional methods, especially for detecting thin vessels and effectively dealing with noise. The Gumbel probability distribution function [5] was utilized to create a unique method for improving vessel detection. This method approximates the probability distribution of vessel pixels, which improves sensitivity and specificity in detecting vessels from the background.

An active contour model has also been created to segment and measure retinal vessels [6]. This technology uses energy minimization techniques to accurately capture the complicated geometries of vessels and offer consistent measurements of vessel diameters, which is critical for identifying disorders like as diabetic retinopathy and glaucoma. The optic disc is an important component in retinal pictures, acting as a reference point for analyzing other retinal structures. The precise localization of the optic disc is critical for diagnosing a variety of eye disorders. The circular Hough transform combined with the grow-cut algorithm [7] is an effective way of identifying and segmenting the optic disc. The circular Hough transform detects the optic disc's round shape, but the grow-cut approach enhances segmentation by including pixel-level information. This method is reliable, and functioning well even in pictures with fluctuating lighting circumstances. Another

option for optic disc localization is to use automatic thresholding methods on morphologically processed Fundus images [8]. Morphological techniques improve the optic disc region, and thresholding is then used to precisely segment the optic disc. This approach has demonstrated efficacy in both normal and diseased instances.

Detecting exudates in retinal images is crucial for diagnosing diabetic retinopathy, one of the leading causes of blindness. An automated exudate identification technique that combines contrast enhancement, noise reduction, and morphological procedures has shown great sensitivity in detecting exudate patches [9]. This approach is useful for detecting diabetic retinopathy early on and allows for prompt treatments. To detect hard exudates, another technique employs dynamic thresholding and support vector machine (SVM) classification [10]. The SVM classifier improves the accuracy of discriminating exudates from other retinal characteristics, while dynamic thresholding adjusts to changing illumination conditions. This method has demonstrated good accuracy and reliability, qualifying it for clinical usage.

Chapter 3 Methodology

3.1 System Design

3.1.1 Optic Disc Localization System Diagram

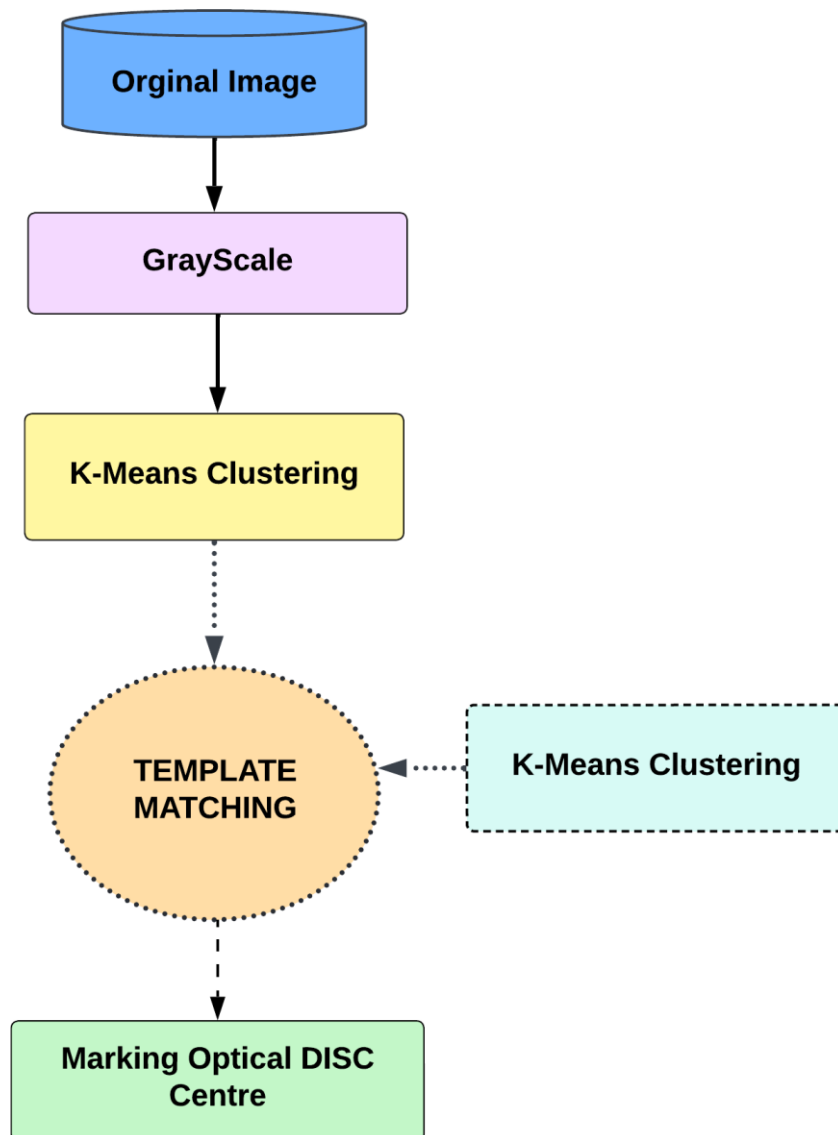


Fig. 2: Optic Disc Localization Flow Diagram

3.1.2 Exudates Detection System Diagram

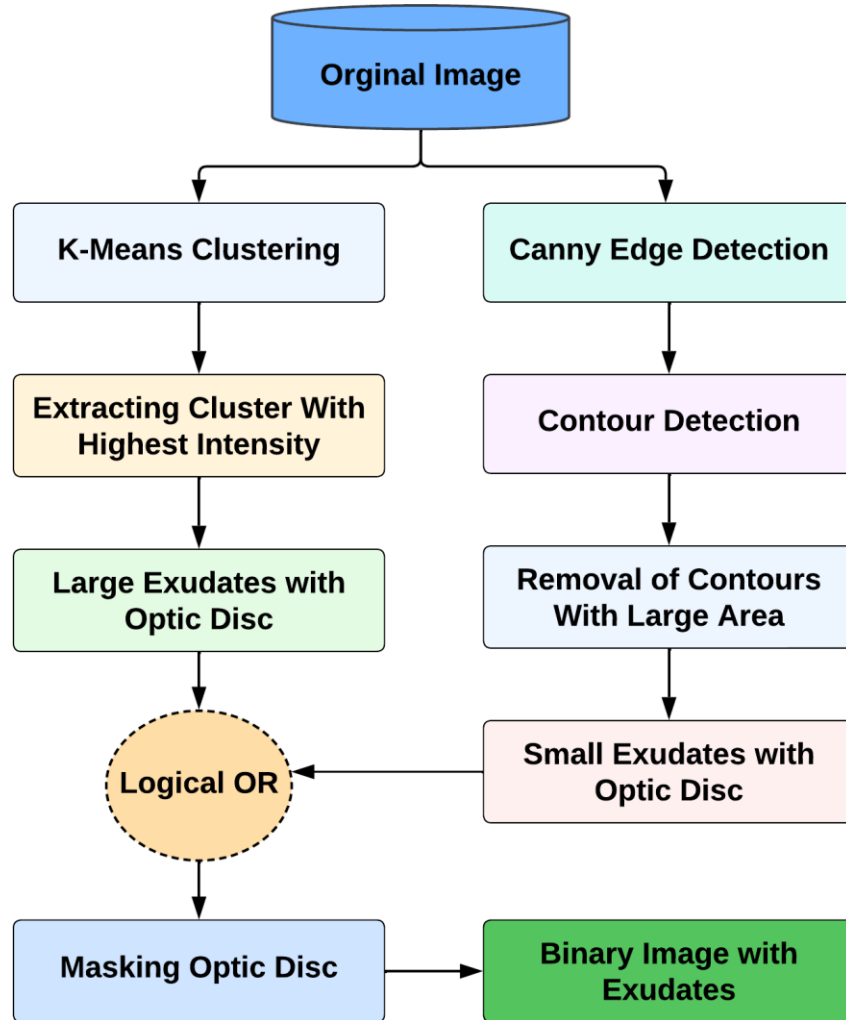


Fig. 3: Exudates Detection Flow Diagram

3.1.3 Blood Vessel Segmentation System Diagram

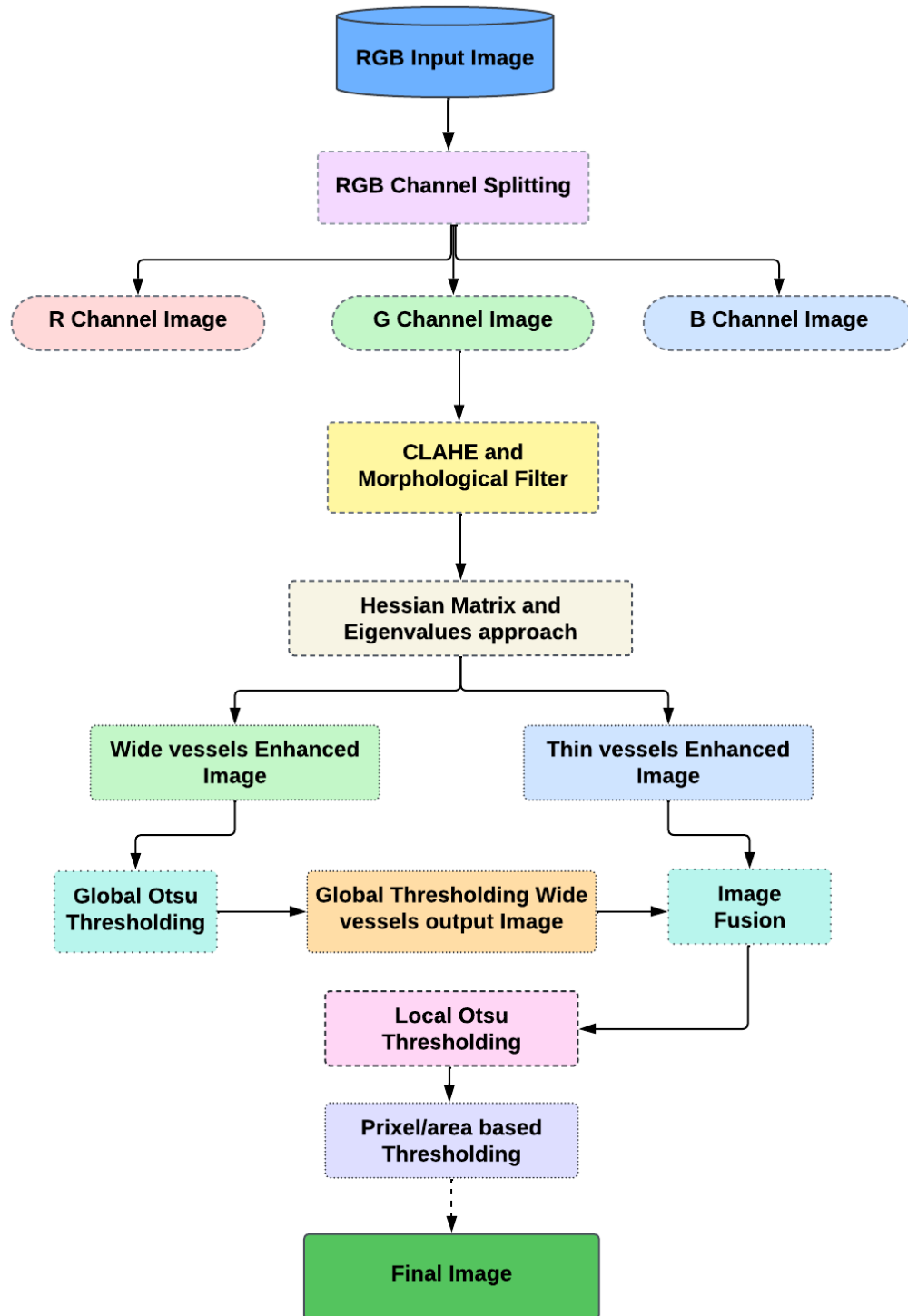


Fig. 4: Segmentation Diagram

3.1.4 Data collection

Dataset part 01 (Optic Disc Localization & Hard Exudates detection)

For the Localization of Optic Disc and detection of Hard Exudates a publicly available dataset the IDRID Segmentation dataset was used. The dataset consists of 81 images. The height and width of each image are $4288\text{px} \times 2848\text{px}$. And the data set was splitted into train set and test set, 54 for train and 27 for test respectively.

Dataset part 02 (Segmentation of Blood Vessels)

For vessel segmentation STARE dataset was used which contained a full 400 raw images. Among those images a total of 44 images were annotated by experts. A total of 44 possible manifestations were queried to the experts during data collection and then reduced to 39 values during encoding. Used for training purposes and the rest of the dataset was used for testing.

3.2 Hardware and/or Software Components

Component	Details
Programming Language	Python (version 3.6.9)
Libraries	OpenCV, Scikit-learn, TensorFlow, Keras
Development Environment	Jupyter Notebooks
Execution platform	Google Collaboratory (standard runtime)
CPU	Intel® Xeon single core, 2.3 GHz
RAM	approximately 12.5 GB
GPU for DCNN Training	Tesla K80 (GPU runtime)

Table 1: Hardware/Software components

Tool	Functions	Other similar tools (if any)	Why selected this tool?
Python	Programming language	TensorFlow, R, NumPy, Pandas	Python is a versatile programming language that is well-suited for deep learning. It is also relatively easy to learn and use.
GPU	Accelerates deep learning computations	CPU, TPU	GPUs are specialized processors that are well-suited for parallel computing tasks, such as deep learning.
TensorFlow	Deep learning framework	PyTorch, JAX, MXNet	TensorFlow is a popular deep learning framework that is known for its ease of use and flexibility.
Keras	High-level API for TensorFlow	PyTorch Lightning, Gluon	Keras is a high-level API for TensorFlow that makes it easier to build and train deep learning models.
Kaggle	Online data science and machine learning platform	GitHub, TopCoder, HackerRank	Kaggle provides access to a large dataset of labelled retinal fundus images, which is essential for training a deep learning model. It also provides a community of data scientists and machine learning experts who can help with the project.
Google Collaborate Pro	Cloud-based Jupyter Notebook Environment	Google Cloud Platform, AWS SageMaker, Azure Machine Learning Studio	Google Collab Pro provides access to powerful GPUs and TPUs, which are essential for training deep learning models. It also provides a convenient way to share and collaborate on projects.

Table 2: List of Software, Libraries and other's Tools

3.3 Hardware and/or Software Implementation

3.3.1 Localization of Optic Disc

Proper localization of the optic disc (OD) is a crucial step in segmenting exudates from fundus images due to the similar gray intensity levels shared by the OD and exudates. The main distinction lies in the irregular shape and generally smaller size of the exudates. In the proposed method, a colored fundus image is first resized to 300×300 pixels. Then, k-means clustering is applied to its grayscale version (Fig. 5c). The k-means algorithm works by minimizing the squared differences between '**k**' cluster centers (or means) and the corresponding pixel values (color values) in the image.

If \mathbf{X}_i represents the i^{th} cluster center and \mathbf{P}_j represents the color value of the j^{th} pixel, the squared error function **JSE** that k-means aims to minimize can be expressed as:

$$J_{SE} = \sum_{i=1}^k \sum_{j=1}^n (||\mathbf{X}_i - \mathbf{P}_j||)^2$$

A template with a size similar to the average OD size across all images was created (Fig. 5d) and then matched with the image using the Normalized Correlation Coefficient (NCCOEFF) method (Fig. 5e). The NCCOEFF is calculated as:

$$\mathbf{R}_{(x,y)} = \frac{\sum_{x',y'} (\mathbf{T}'(x',y') \cdot \mathbf{I}'(x+x',y+y'))}{\sqrt{\sum_{x',y'} \mathbf{T}'(x',y')^2 \cdot \sum_{x',y'} \mathbf{I}'(x+x',y+y')^2}}$$

The position corresponding to the maximum values from the template-matching result was identified, which approximates the center of the Optic Disc in the image (Fig. 5f). The steps of the algorithm are illustrated in Fig. 5.

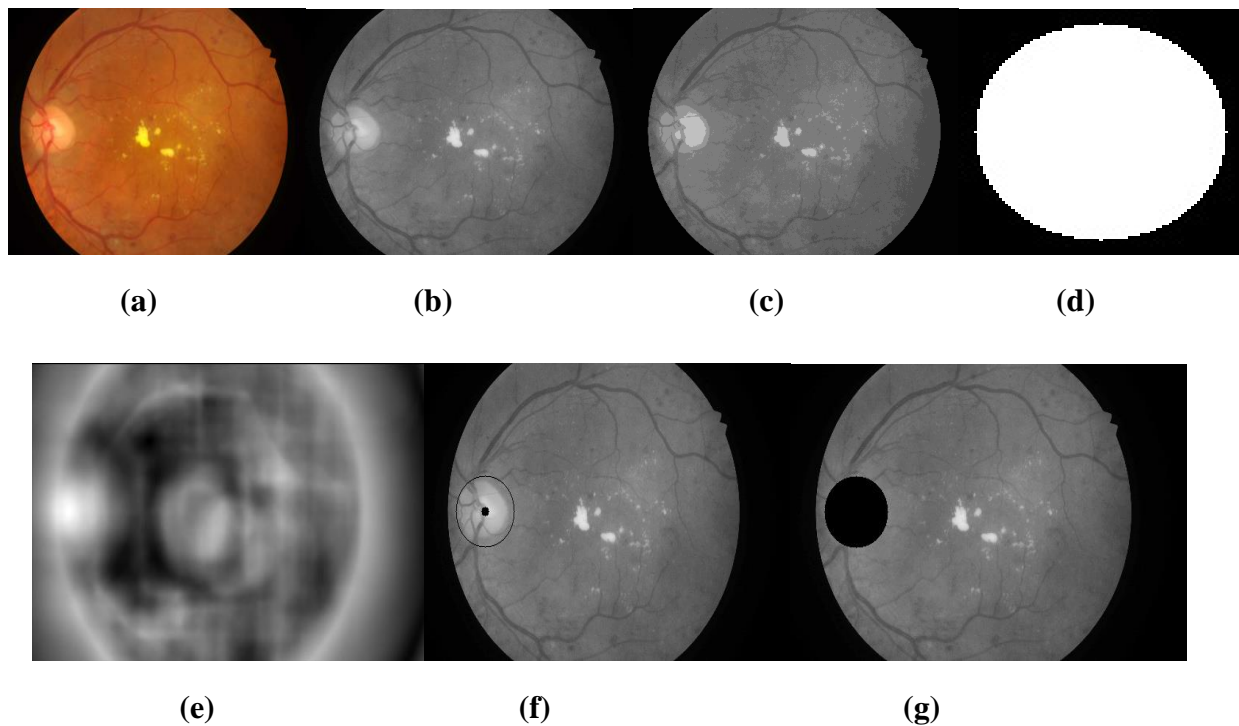


Fig. 5: (a) Original image, (b) Grayscale of (a), (c) Result of *k*-means clustering, (d) Generated Template, (e) Template Matching result (using *NCCOEFF*; notice the OD region has highest similarity), (f) Marking OD and its center, (g) Masking OD region.

3.3.2 Detection of Exudates

Sometimes protein leakage occurs from the retinal vessels resulting in yellowish deposits of protein located on the outer layer of the retina. These small yellowish deposits are called Exudates.

To find hard exudates initially the original picture shown in the picture (Fig. 6b) was subjected to *k*-means clustering. And the cluster with the greatest intensities was selected and binarized. This removes the OD and all of the exudates, including the biggest ones (Fig. 6c). The green channel picture was then subjected to a consecutive application of Canny Edge and Contour detection in order to remove big structures. Later on, pixels with maximum gray level intensities were considered to create a binary image applying an appropriate thresholding. Which helped extraction of small exudates with the OD. Then the images containing the small and large exudates were logically added (Fig. 6d). In order to get the final segmentation result shown in (Fig. 6e) The

aforementioned method was used to detect OD in grayscale images and a circular, black mask was placed over the grayscale image. The algorithm's steps are shown in the system diagram (Fig. 6e).

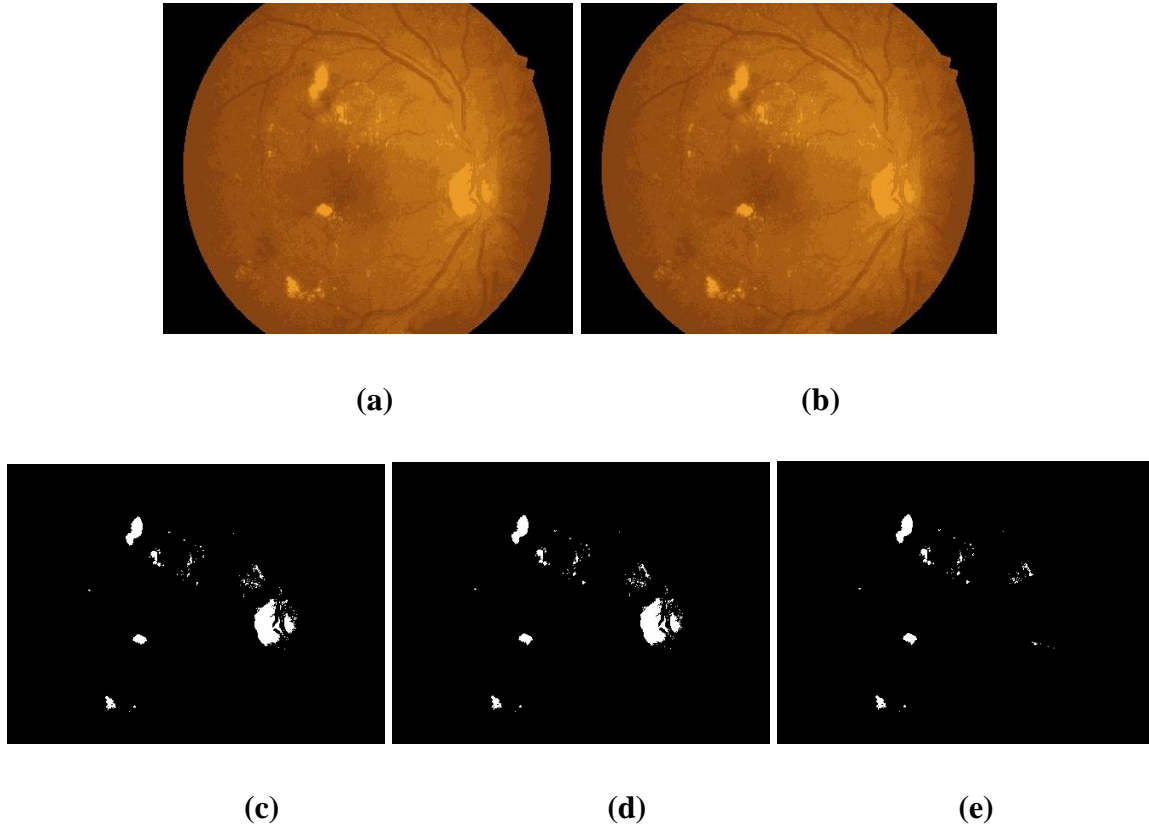


Fig. 6: (a) Original Image, (b) K-means clustering result, (c) Extracting the exudates from (b) and thresholding, (d) Logical OR of (c) and the images containing the smallest exudates, (e) Final segmentation result after OD masking.

Binary Diagnosis of Diabetic Retinopathy using Deep Convolutional Neural Network. The following DCNN was developed for the binary classification of DR.

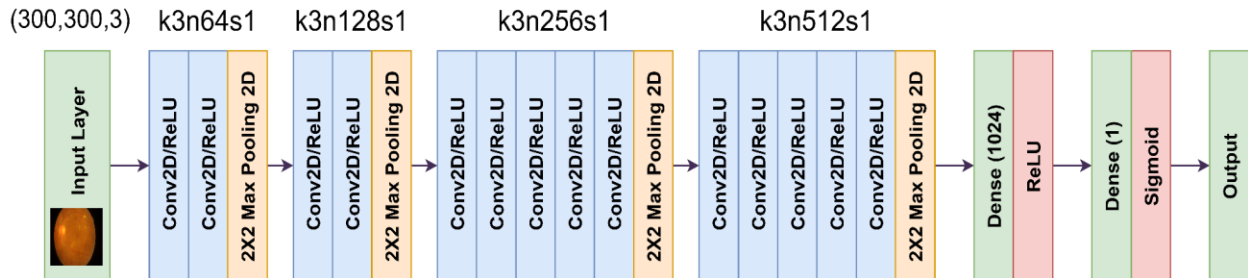


Fig. 7: DCNN architecture with the corresponding kernel/filter sizes (k), number of feature maps (n) and strides (s) specified for each convolutional layer.

In order to perform DR diagnosis this proposed DCNN architecture was adapted from VGG-16 model architecture. This architecture is composed of 4 stages of convolutional layers. Between each of those layers a 2x2 2D max pooling layers are composed. which helped down sampling the input image by a factor of 2. Small 3x3 kernels with the Rectified Linear Unit (ReLU) was used as the activation function in each convolutional layer.

$$\text{ReLU}(x) = \max(0, x), \quad x \in R$$

Again, the colored original photos are scaled to 300 x 300 pixels and trained using an 8-batch size. After that the resized output image is fed to a fully connected layer with 1024 neurons as well as to ReLU activation function. The last layer consists of a single neuron that has the binary classification Sigmoid activation function, shown in the equation below.

$$S(x) = \frac{1}{1 + e^{-x}}$$

The network was optimized using the Adam optimizer, it has a learning rate of 0.0001 and Binary Cross Entropy loss JBCE, shown in this equation below.

$$J_{BCE} = -\frac{1}{m} \sum_{i=1}^m y_i \cdot \log(p(y_i)) + (1 - y_i) \cdot \log(1 - p(y_i))$$

In the above equation y_i is the actual label, $p(y_i)$ is the predicted probability of y_i and m is the number of training/test examples.

3.3.3 Vessel Segmentation

- **RGB image input and RGB Channel Splitting:**

The RGB (Red, Green, Blue) color model commonly represents colors in digital images. These three channels' intensity values are stored in each pixel of an image, and the combination of these values yields the final color we see. By splitting an RGB image, these

channels may be individually analyzed or manipulated as separate grayscale images.

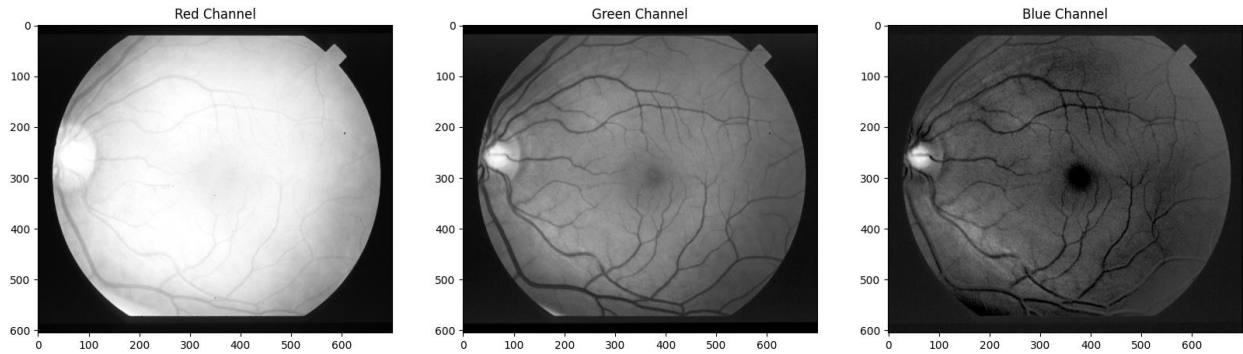
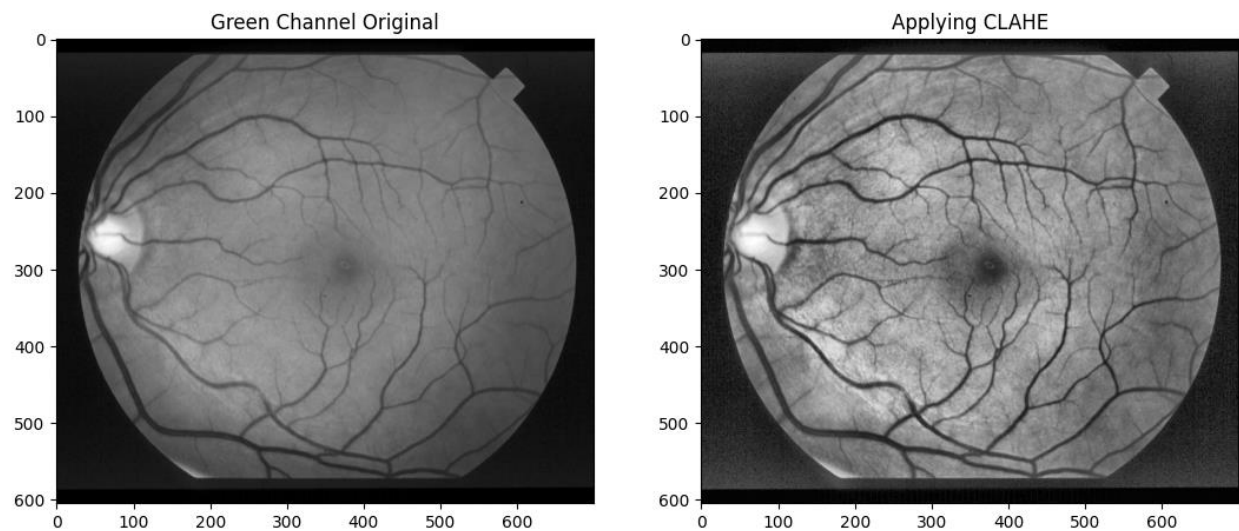


Fig. 8: RGB Channel Splitting

- **CLAHE and Morphological Filter:**

After using RGB channel splitting, we used CLAHE and morphological filters. CLAHE is an image processing technique that we use to improve the contrast of images, particularly those with uneven illumination, such as contrast enhancement, adaptive, and contrast limited. Then, we used Morphological filters, a set of image processing techniques used for shape analysis, noise reduction, and edge detection.



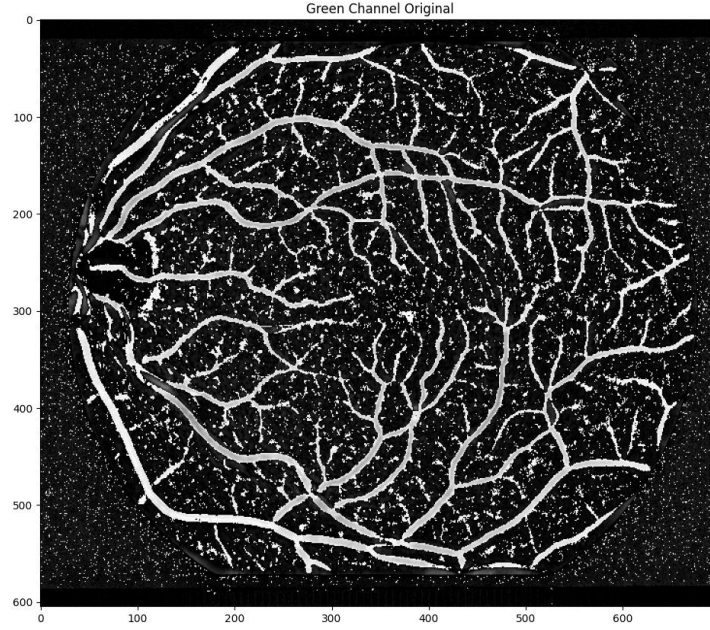


Fig. 9: Applying CLAHE and Morphological Filter

- **Hessian Matrix Eigenvalues based approach:**

We used the hessian matrix and eigenvalue transformation uniquely after morphological filtering to produce improved images of wide and thin blood vessels. Actually, the Hessian Matrix represents the local curvature of an ocular image at a specific pixel. It is calculated using second-order partial derivatives of the ocular image intensity. We used the Hessian matrix's eigenvalues to determine which pixels are most likely blood vessel pixels. Positive eigenvalues in one direction and negative eigenvalues in the opposite direction are prime candidates for vessel pixels. This characteristic enabled us to distinguish the network of blood vessels from the background retinal tissue.

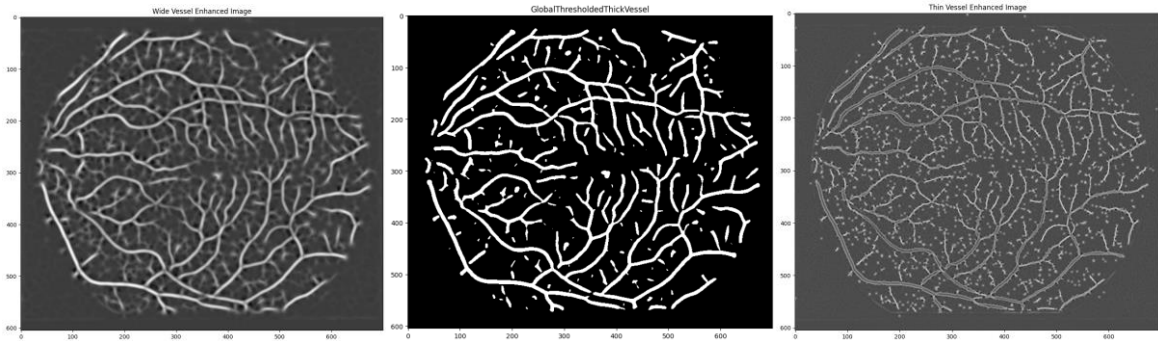


Fig. 10: Applying Hessian Matrix

- **Image Fusioning:**

We have combined the global threshold thick vessel image with thin vessel enhanced image to create a fusion image.

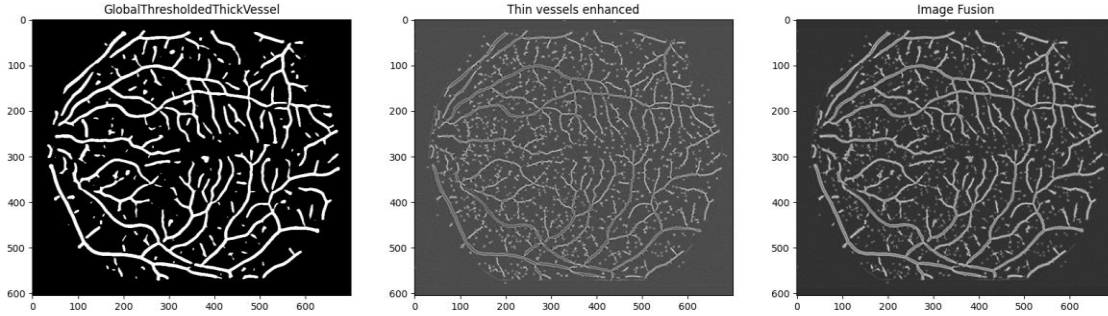


Fig. 11: Image Fusioning

- **Local Otsu Thresholding method for vessel segmentation**

We employed the local Otsu thresholding approach for vessel segmentation, a more advanced method that increases vessel visibility while reducing noise and unnecessary objects. Instead of using Otsu's approach on an entire image, it is applied separately to wide and thin vessel images. Initially, the wide vessel-enhanced image is put through to a global threshold, and the outcome is then combined with the thin vessel-enhanced image. The threshold is then adjusted via local thresholding depending on the position of the vessel. To extract small or thin vessels, a lower threshold is established for regions away from wide vessels, and an offset is given to the global threshold to decrease noise surrounding wide vessels.

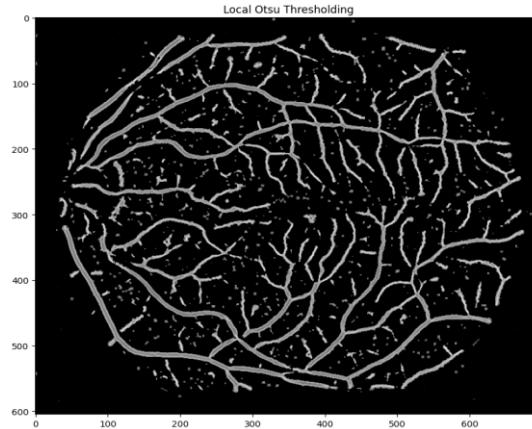


Fig. 12: Local Otsu thresholding

- **Pixel area-based Thresholding:**

Then, pixel area-based thresholding removes any pixels below a threshold area (30px) to remove any unnecessary pixels and unconnected non-vessel pixels to clarify only the connected vessels that provide us with the final segmented image.

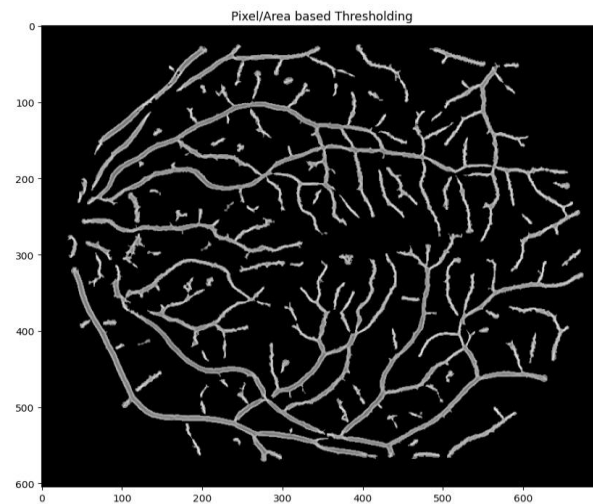


Fig. 13: Pixel area-based Thresholding

Chapter 4 Investigation/Experiment, Result, Analysis, and Discussion

4.1 Investigation/Experiment

In this chapter, we present the experiments conducted to achieve segmentation of blood vessels, optic disc localization, detection of exudates for diabetic retinopathy, and glaucoma diagnosis from fundus images. We describe the methodologies employed, the data used, the variables considered, and the results obtained. Finally, we provide a discussion on the outcomes of these experiments, comparing them with the state-of-the-art techniques.

4.2 Result

4.2.1 Localization of Optic Disc

The proposed Optic Disc Localization algorithm successfully identified the OD in 80 out of 81 images in the entire dataset, resulting in an accuracy of 98.77%.

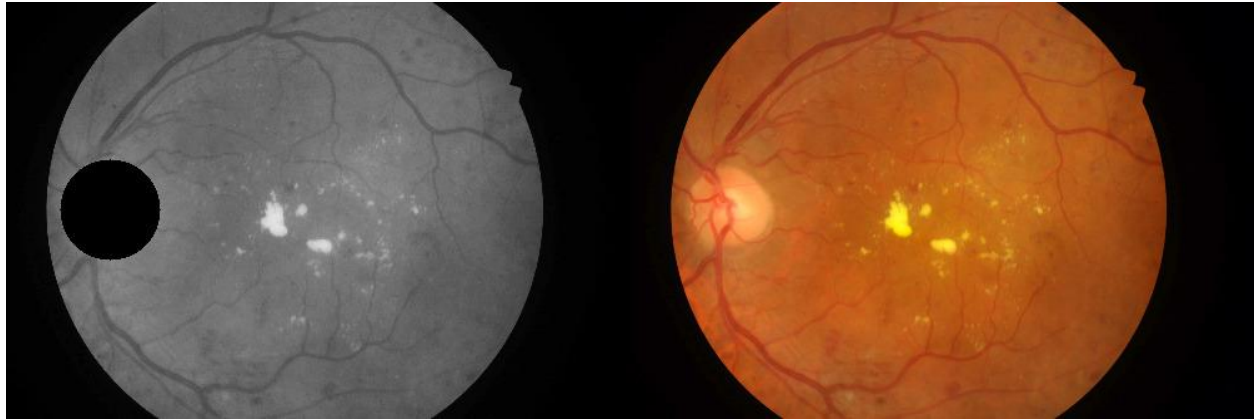
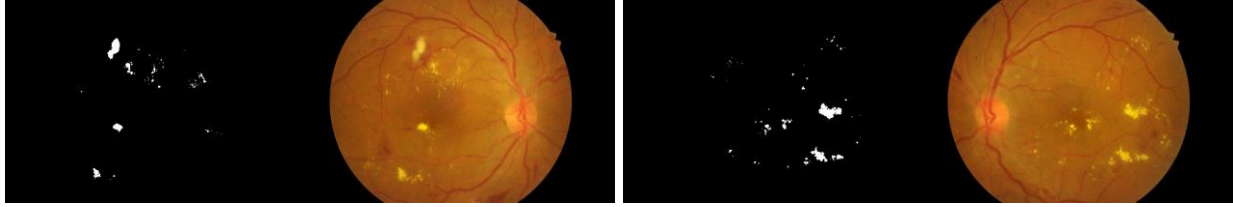


Fig. 14: Optic Disc masked image (left) with the original image (right)

4.2.2 Detection of Exudates

The proposed algorithm successfully detected exudates in all 81 images from the IDRiD Segmentation dataset with a high level of accuracy.



(a)

(b)

Fig. 15: (a), (b) Result of proposed exudate detection method (left) with original image (right).

4.2.3 Segmentation of blood vessels

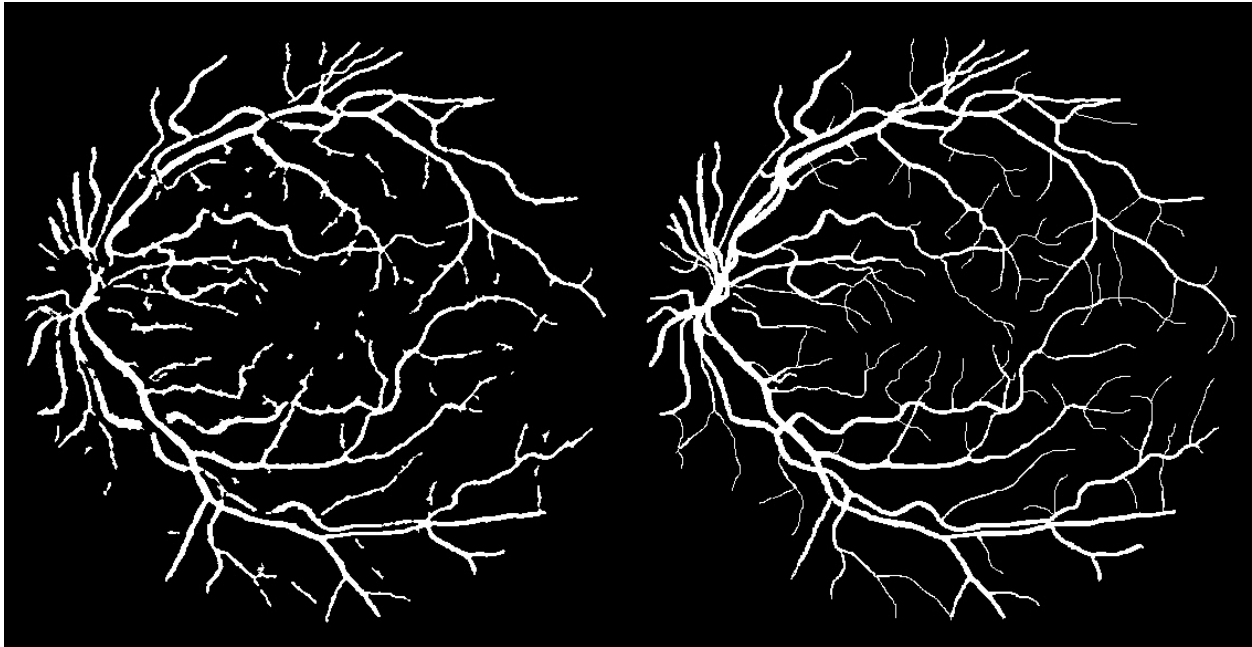


Fig. 16: Segmentation result for the best case (left) with ground truth (right)

Images	State Dataset		
	Accuracy	Sensitivity (Sn)	Specificity (Sp)
1	0.942	0.714	0.961
2	0.943	0.601	0.968
3	0.916	0.833	0.922
4	0.813	0.868	0.810

5	0.952	0.750	0.972
6	0.962	0.806	0.974
7	0.955	0.840	0.966
8	0.961	0.796	0.974
9	0.955	0.829	0.966
10	0.961	0.775	0.977
11	0.964	0.650	0.988
12	0.971	0.834	0.982
13	0.957	0.701	0.982
14	0.958	0.715	0.983
15	0.954	0.770	0.972
16	0.941	0.645	0.974
17	0.967	0.806	0.983
18	0.976	0.604	0.996
19	0.924	0.858	0.943
20	0.945	0.766	0.961
Average	0.94585	0.75805	0.9627

Table 3: Results of the proposed vessel segmentation method on the STATE dataset

4.3 Analysis

The suggested Optic Disc (OD) localization approach accurately detected the OD in 98.77% of images. This approach uses k-means clustering on the grayscale picture to efficiently recognize the OD from other structures based on its distinct profile and contrast. The exceptionally high accuracy gained demonstrates the strength of the k-means clustering strategy combined with template matching, making it a dependable technique for OD localization.

The blood vessel segmentation algorithm performs exceptionally well, surpassing many existing methods. The algorithm provides precise segmentation of blood vessels by utilizing morphological operations and thresholding techniques. The noise reduction techniques built into the methodology are critical for reducing false positives and increasing accuracy. This method enables a more precise study of blood vessel patterns, which is essential for identifying various retinal disorders.

Exudates were successfully detected across every image in the IDRiD Segmentation dataset. Exudates are successfully separated from other features in the image by using k-means clustering to find high-intensity areas, followed by Canny Edge and contour detection. Integrating exudates and OD detection may occasionally make it difficult to distinguish between them. Still, the combination of both approaches ensures that both big and tiny exudates are reliably recognized. The final step, masking the OD, helps refine the segmentation results.

The DCNN model, which had 14 convolutional layers and two fully linked layers, attained a diagnosis accuracy of 75.73%. While this accuracy is impressive, it identifies areas for further development. DCNNs are often more resilient to noise and can detect complicated patterns in data. However, gaining better accuracy may require additional network design optimization, training parameters, and more varied training data. The current performance indicates a strong foundation, but there is still space for improvement and refining.

Compared to existing approaches, the suggested OD localization and blood vessel segmentation strategies have much higher accuracy and reliability. Combining morphological processes and sophisticated clustering techniques allows for more exact segmentation of blood vessels, while the k-means-based OD localization approach produces consistent results. The DCNN model's performance meets expectations, although future tweaks might improve its diagnostic skills.

4.4 Discussion

The new techniques for analyzing fundus images show significant improvements in automatically diagnosing diabetic retinopathy (DR). The method for localizing the optic disc (OD) achieved a high accuracy of 98.77% using effective k-means clustering and template matching, demonstrating its reliability. Blood vessel segmentation using advanced morphological operations and thresholding surpassed existing techniques, providing precise results important for DR diagnosis. Exudate detection successfully isolated exudates despite challenges with overlapping features, using a combination of k-means clustering, Canny Edge, and Contour detection. The Deep Convolutional Neural Network (DCNN) achieved a diagnostic accuracy of 75.73%, showing potential for improvement. Overall, these methods represent significant advancements in feature extraction and DR diagnosis, with the need for future work to optimize the DCNN and explore additional techniques for better performance.

Chapter 5 Conclusions

8.1 Summary

In this report, a new method for segmenting blood vessels in retinal images is introduced. Our approach combines contrast-limited Adaptive Histogram Equalization (CLAHE) with morphological filters to improve the visibility of blood vessels and eliminate unwanted noise. Advanced techniques like the Hessian matrix and eigenvalue transformations are then utilized to categorize the images into wide and thin vessel categories. To extract vessel features, we employ Otsu thresholding and region-based thresholding to determine the optimal value for distinguishing vessel pixels from non-vessel pixels. This method was tested on various datasets, including STARE, and its sensitivity, specificity, and accuracy performance were evaluated. Compared to other methods, our approach excels in its ability to handle noise and accurately extract thin vessels. While deep convolutional neural networks (DCNNs) typically offer better sensitivity and noise resistance, our method is effective because it focuses on the vessel structure rather than intensity. However, it may occasionally mistake the optic disc (OD) for large exudates when their sizes are similar. Our exudate detection algorithm is designed to identify both large and small exudates, but it may occasionally produce false positives in poorly illuminated images. The DCNN model we propose can be trained in approximately an hour on Google Collab and achieves a test accuracy of 75.73%, outperforming many previous models and offering the advantage of faster training times.

8.2 Limitations

Despite its advantages, the suggested technique has several drawbacks that should be considered:

- **Difficulty Distinguishing Between OD and Exudates** When the optic disc (OD) and big exudates are of comparable size, the technique may need to help distinguish between them. While it correctly detects the OD based on its size and structure, this method might be confusing when a big exudate closely resembles the OD in size.
- **False Positives in Uneven Illumination:** Although the exudate identification algorithm can detect big and tiny exudates, it can cause false positives in images with uneven illumination. Lighting variations can impact the algorithm's ability to identify and categories exudates correctly.

These limitations highlight areas for potential improvement and further research to enhance the robustness and accuracy of the proposed method.

8.3 Future Improvement

- **Enhanced Optic Disc and Exudate Differentiation:** Future work could focus on developing more sophisticated algorithms to better differentiate between the optic disc (OD) and exudates, especially when their sizes are similar. Integrating advanced machine learning techniques or including additional image features such as texture or color may improve the accuracy of this differentiation.
- **Improved Handling of Uneven Illumination:** In order to decrease the number of incorrect detections in images with uneven lighting, we can consider using advanced illumination correction techniques or adaptive thresholding methods. These enhancements will enable the algorithm to produce more reliable results under different lighting conditions.
- **Integration of Advanced DCNN Architectures:** Even though the current DCNN architecture provides a good balance between training time and accuracy, there is potential for further improvement in sensitivity and overall accuracy by exploring more advanced and deeper network architectures. Techniques such as transfer learning or hybrid models that combine traditional image processing with deep learning could be considered.

References

1. Yau JW, Rogers SL, Kawasaki R, et al Global prevalence and major risk factors of diabetic retinopathy. *Diabetes Care* 2012; 35:556–64.
2. Tham YC, Li X, Wong TY, et al Global prevalence of glaucoma and projections of glaucoma burden through 2040: a systematic review and meta-analysis. *Ophthalmology* 2014; 121:2081–90.
3. Wang, S. et al.: “Hierarchical retinal blood vessel segmentation based on feature and ensemble learning.” *Neurocomputing* 149: 708-717 (2015).
4. Zhang, L., Fisher, M., Wang, W.: Retinal vessel segmentation using multi-scale textons derived from keypoints. *Comput Med Imaging Graph.* 45:47–56 (2015).
5. Singh, N.P., Srivastava R.: Retinal blood vessels segmentation by using Gumbel probability distribution function based matched filter. *Comput Methods Programs Biomed* (2016).
6. Al-Diri, B., Hunter, A., Steel, D.: An active contour model for segmenting and measuring retinal vessels. *IEEE Trans Med Imaging.* 28(9):1488–97 (2009).
7. Abdullah, M. et al.: Localization and segmentation of optic disc in retinal images using circular Hough transform and grow-cut algorithm. *PeerJ*; 4: e2003 (2016).
8. Mary, M.C.V.S. et al. An empirical study on optic disc segmentation using an active contour model. *Biomedical Signal Processing and Control.* 18:19–29 (2015).
9. Abbadi, N.K., Al-Saadi, E.H.: Automatic Detection of Exudates in Retinal Images (2013).
10. Marin, D., Gegundez-Arias, M.E., Suero, A., Bravo, J.M.: Obtaining optic disc center and pixel region by automatic thresholding methods on morphologically processed fundus images. *Comput Methods Programs Biomed.* 118(2):173-185 (2015).